NUMERICAL SIMULATION OF BLOWING PROCESS IN THE OVERAGING SECTION OF A VERTICAL CONTINUOUS ANNEALING FURNACE USING CFD

Peng GAO[1], Shengyou CHEN[1], Shixian LAI[1], Jian WANG[2], Guangji XU[3], Chaoyang SUN[1], Shaochuan FENG[1*]

[1] School of Mechanical Engineering, University of Science and Technology Beijing, Beijing 100083, China

[2] Research Institute, Baoshan Iron & Steel Co., Ltd., Shanghai 201900, China

[3] Cold Rolling Mill, Baoshan Iron & Steel Co. Ltd., Shanghai 200941, China

[*] Corresponding author; Email address: fengshaochuan@ustb.edu.cn

The vertical continuous annealing furnace plays a pivotal role in the annealing treatment line of strip steel. Within this furnace, expelling the air by blowing protection gas is essential. This helps reduce the oxygen content, thereby preventing the formation of oxides and impurities on the surface of the strip steel. This study aims to investigate the influence of the structure of the overaging section of a vertical continuous annealing furnace on the blowing effect. The gas flow characteristics during the blowing process have also been examined, revealing the location and distribution of stagnant zones. Computational fluid dynamics (CFD) is used to solve a three-dimensional (3D) simulation model numerically, calculating the flow and velocity of gas within the furnace for blow times ranging from 0 to 100 seconds. The results indicate that the flow field in the furnace reaches a quasi-steady state at a blow time of approximately 75 seconds. However, the issue of flow field voids and stagnant zones shows negligible improvement beyond this point. The blowing effect varies across different regions of the furnace, with a notable area of flow field void and stagnant zone in the lower part of the furnace, far from the furnace throat, resulting in a suboptimal blowing effect. The findings of this study can serve as valuable guidance for optimizing the internal structure of a vertical continuous annealing furnace and improving the efficiency of the blowing process.

Key words: *Vertical continuous annealing furnace; Overaging section; Velocity field; Numerical simulation; Stagnant zone*

1. Introduction

Annealing is a critical process in the production of cold-rolled strip steel. It is primarily aimed at improving surface quality, relieving internal stresses, extending fatigue life, and enhancing the processing performance of strip steel [1–3]. The rolled steel must undergo a process of recrystallization annealing to eliminate cold work hardening after rolling [4–6]. Although the hardness and strength of cold-rolled strip steel decrease after annealing, its ductility, toughness, and plasticity significantly

improve, and cutting performance is enhanced [7,8]. Therefore, the annealing treatment can enable the production of cold-rolled strip steel with exceptional processability and usability. A vertical continuous annealing furnace represents a collaborative manufacturing line for the annealing process of cold-rolled strip steel in the steel industry. The primary function of this process is to elevate the strip steel to the specified annealing temperature and then systematically lower it to attain the precise temperature required for the recrystallization annealing of cold-rolled strip steel [9,10]. The continuous annealing process for cold-rolled strip steel usually involves several stages, including heating, soaking, cooling, and overaging [11,12]. The vertical continuous annealing furnace studied in this paper is comprised of eight primary sections: preheating, heating, uniform heating, slow cooling, rapid cooling, overaging, final cooling, and water quenching cooling [13].

In the continuous annealing process of strip steel, a nitrogen and hydrogen gas mixture serves as the protective gas, introduced into the furnace via blowing pipes and forming a gas jet. The gas jet cooling enables heat exchange with the strip steel while expelling air [14]. The primary objective is to diminish the oxygen content within the furnace, thereby mitigating the formation of oxides and impurities on the strip steel surface. As such, the introduction of protective gas into the furnace plays a critical role in governing the quality of the final strip steels. The content of protective gas in the furnace is directly impacted by the flow and temperature fields within the furnace, both of which are subject to factors such as furnace structure, blowing methods, and strategies.

The flow of fluid within a cavity is usually a complex turbulent issue, and computational fluid dynamics (CFD) is the primary method used to analyze this problem [2,6]. In the investigation of heat and mass transfer within a continuous annealing furnace, Han et al. examined the heating characteristics of the slab in a bench-scale reheating furnace using a computational fluid dynamics (CFD) model based on the finite volume method (FVM) [15]. To address the intricacies of the flow field, the researchers utilized the standard k-ε model to solve the turbulent flow. Chen et al. developed mathematical and physical models utilizing computational fluid dynamics (CFD) and neural network methodologies to forecast the temperature of strip steel in continuous annealing furnaces [16]. Subsequently, they conducted numerical simulations and observed that the CFD model yielded superior computational precision in contrast to the neural network models. Notably, the predictions derived from the models aligned consistently with the empirical data. Hajaliakbari and Hassanpour meticulously calculated the total heat absorbed by strip steel and conducted an in-depth analysis of the impact of process parameters such as strip width, thickness, speed, heating power generated by radiation tubes, and its distribution on the overall efficiency of continuous annealing furnaces using a comprehensive mathematical model [10]. Zareba et al. conducted a mathematical model for a horizontal continuous annealing furnace, and the temperatures of strip, gas, and wall are calculated considering the convective and radiative heat transfer [17].

The overaging treatment constitutes a critical procedure in the cooling phase of continuous annealing for strip steel. This process is designed to augment the quantity of granular retained austenite and improve the yield strength and elongation of the strip steel [18–20]. The section relating to overaging in a particular type of vertical continuous annealing furnace that has been examined in this paper predominantly encompasses the furnace throat, guide roller, bellows, blow tube, air inlet, and outlet. Among these components, the bellows comprise multiple blowing pipes equipped with several small round holes oriented towards the side of the strip steel. These holes serve as inlets for injecting protective gas into the furnace. The outlet has a simple structure: a square opening on the side of the furnace wall

away from the air inlet. Because of numerous protruding structures and angles inside the furnace, gas flow is hindered, resulting in inadequate and non-uniform blowing of protection gas and ultimately leading to elevated oxide content and compromised surface quality of the strip steel [21].

The analysis of flow field characteristics and investigation of the impact of stagnant zones in the furnace play a vital role in enhancing the performance of strip steel products. This paper presents the construction of a geometric model of the overaging section of a vertical continuous annealing furnace based on the provided drawing. A numerical model employing the CFD method is utilized to address the flow field, with specific attention devoted to the analysis of stagnant zones affecting the content and uniformity of the protective gas.

2. Model building and simplification

The research paper investigates the blowing process within the overaging section of the vertical continuous annealing furnace. This process involves the use of bellows, which are comprised of several rows of blowing pipes. Each blowing pipe is fitted with regularly spaced air holes, allowing protective gas to flow through and form impinging jets. These jets swiftly move toward the surface of the strip steel, displacing the blowing atmosphere inside the furnace and facilitating heat exchange with the strip steel. The three-dimensional geometric model of the overaging section in the vertical continuous annealing furnace, excluding the strip steel, was constructed using SolidWorks. This model, as depicted in fig. 1, illustrates the internal structure and overall dimensions of the section. In fig. 1, the direction of the strip steel's movement is from the lower left furnace throat to the upper right furnace throat. The furnace chamber comprises six main components: guide rollers, bellows, side wall tubes, heating tubes, support frames, and outlets. The heating tubes are exclusively used to preheat the furnace temperature during the start-up phase. Typically, the overaging section of the vertical continuous annealing furnace is a large-sized cavity structure, with a distance from center to center between the top and bottom guide rollers of 22.08 meters, a depth of 2.5 meters, side wall thickness of approximately 0.2 meters, and front and rear wall thicknesses of about 0.25 meters. However, some small structures and components (less than 0.01 meters) are still present inside the furnace. The difference between the maximum and minimum dimensions of the furnace structure is up to 104 times, posing significant challenges for mesh discretization in numerical simulation. When building a CFD numerical model, it is important to ensure that the mesh size is smaller than the minimum structure size to avoid significant errors. During the overaging stage of a vertical continuous annealing furnace, the presence of small-sized structures and components results in smaller grid sizes and a greater number of grids, which can impact computational efficiency and increase costs. Therefore, it is crucial to appropriately simplify the geometric model used for calculations while striving to maintain the accuracy of the results. This article highlights the repetitive periodic pattern in the structure of the overaging section of the vertical continuous annealing furnace, as demonstrated by the blue frame lines in fig. 1. The focus is on simplifying the overall structure by retaining only one cycle and omitting the repetitive parts while preserving basic geometric features. Simplification methods include expanding local feature dimensions and merging periodic array structures for components like the support frame, side wall tube, heating tube, and bellows. Additionally, to enhance efficiency, it is suggested that the number of air holes on the blowing tube be reduced and the diameter of the air holes increased, as shown in fig. 2a and 2b. The simplified geometric model of the vertical continuous annealing furnace aging section is depicted in fig. 2c.
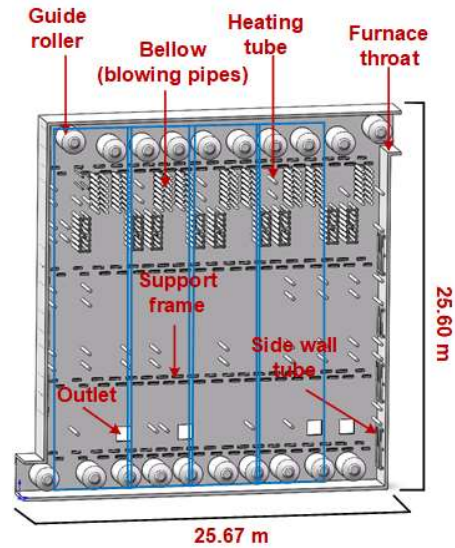
Figure 1. Internal structures and overall dimensions of the overaging section of a vertical continuous annealing furnace
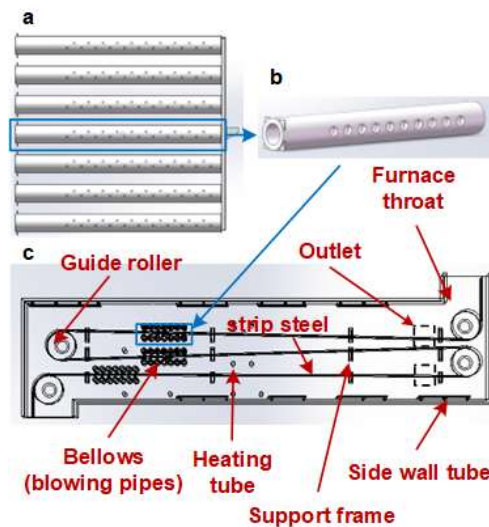

Figure 2. Simplification of the geometric model (taking blowing pipes as an example): (a) structures of the blowing pipes before simplification; (b) structures of the blowing pipes after simplification; and (c) simplified overall geometric model of the overaging section of the vertical continuous annealing furnace

2.1. CFD numerical model

This study focused on the blowing process of the overaging section in a vertical continuous annealing furnace. Utilizing high-precision finite volume-based computational fluid dynamics (CFD) software, FLOW-3D, a mathematical model was built and numerical computation of the gas flow and velocity fields within the furnace was solved. The primary aim was to identify any flow stagnant zones that may impact blowing efficiency and uniformity.

In the process of modeling and solving the equations, the following assumptions were made:

(1)   The motion of the strip steel is neglected by considering it to be in a stationary state.

(2)   The blowing gas is assumed to be an incompressible Newtonian fluid.

The three-dimensional geometric model depicted in fig. 2c is converted to an STL file format and then imported into FLOW-3D. When considering the CFD model, it is important to note that the mesh size has a direct impact on the accuracy of the simulation results. A Cartesian mesh system was implemented with a minimum mesh size of 0.03 m to ensure computational accuracy. Fig. 3a presents the geometric model of blowing pipes before mesh discretization and the mesh system used for discretization, while fig. 3b displays the mesh discretizing results, illustrating the final computational domain.
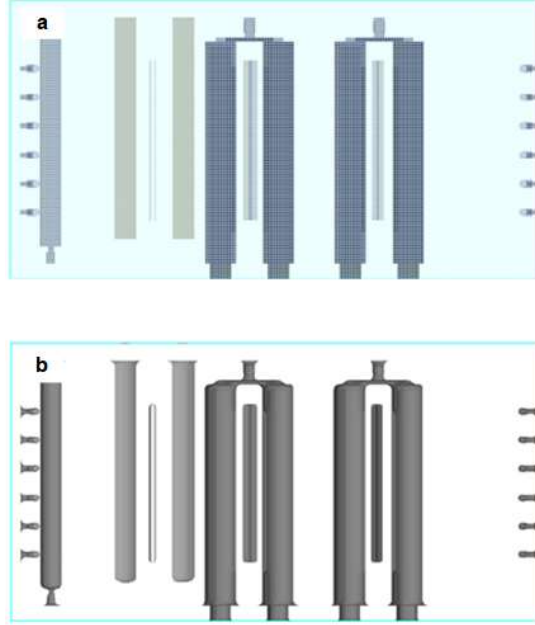

Figure 3. (a) Geometric model of blowing pipes before mesh discretization and mesh system used for discretization; (b) geometric model of blowing pipes after mesh discretization

2.2. Governing equations

The Reynolds-averaged Navier-Stokes equations are utilized to solve for the flow and velocity field of the gas within the furnace [22].
Mass continuity equation：

$$\frac{\partial(uA_x)}{\partial x} + \frac{\partial(vA_y)}{\partial y} + \frac{\partial(wA_z)}{\partial z} = \frac{R_{SOR}}{\rho} \tag{1}$$

Momentum equations：

$$\frac{\partial u}{\partial t} + \frac{1}{V_F}\left(uA_x\frac{\partial u}{\partial x} + vA_y\frac{\partial u}{\partial y} + wA_z\frac{\partial u}{\partial z}\right) = -\frac{\partial p}{\rho\partial x} + G_x + f_x \tag{2}$$

$$\frac{\partial w}{\partial t} + \frac{1}{V_F}\left(uA_x\frac{\partial w}{\partial x} + vA_y\frac{\partial w}{\partial y} + wA_z\frac{\partial w}{\partial z}\right) = -\frac{\partial p}{\rho\partial w} + G_z + f_z \tag{3}$$

$$\frac{\partial v}{\partial t} + \frac{1}{V_F}\left(uA_x\frac{\partial v}{\partial x} + vA_y\frac{\partial v}{\partial y} + wA_z\frac{\partial v}{\partial z}\right) = -\frac{\partial p}{\rho\partial y} + G_y + f_y \tag{4}$$

In the equations, u, v, w are the velocity components in the coordinate directions x, y, z respectively; A_x, A_y, A_z is the friction area open to flow in the x, y, z directions; R_{SOR} is a mass source; ρ is the fluid density;

t is time; V_F is the friction volume open to flow; p is the pressure; G_x, G_y, G_z are body accelerations; f_x, f_y, f_z are vicious accelerations. Due to the complex structure within the furnace, the fluid flow inside the annealing furnace is turbulent, and the standard k-ε two-equation model is employed to solve the fluid flow [23, 24]. Specifically, the transport equations corresponding to turbulent kinetic energy (k) and turbulent kinetic energy dissipation rate (ε) are as follows:

$$\frac{\partial k_T}{\partial t} + \frac{1}{V_F}\left(uA_x\frac{\partial k_T}{\partial x} + vA_y\frac{\partial k_T}{\partial y} + wA_z\frac{\partial k_T}{\partial z}\right) = P_T + G_T + Diff_{k_T} - \varepsilon_T \tag{5}$$

$$\frac{\partial \varepsilon_T}{\partial t} + \frac{1}{V_F}\left(uA_x\frac{\partial \varepsilon_T}{\partial x} + vA_y\frac{\partial \varepsilon_T}{\partial y} + wA_z\frac{\partial \varepsilon_T}{\partial z}\right) =$$
$$\frac{CDIS_1 \bullet \varepsilon_T}{k_T}(P_T + CDIS_3 \bullet G_T) + Diff_\varepsilon - CDIS_2\frac{{\varepsilon_T}^2}{k_T} \tag{6}$$

In the equations, k_T is the turbulent kinetic energy, P_T is the turbulent kinetic energy production, G_T is the buoyancy production term, $Diff_{kT}$ is the turbulent kinetic energy diffusion term, ε_T is the turbulent kinetic energy dissipation, $CDIS_1$, $CDIS_2$, and $CDIS_3$ are empirical constants of the model, with respective values of 1.44, 1.92, and 0.2, and $Diff_\varepsilon$ is the diffusion of dissipation.

2.3. Initial conditions and boundary conditions

The temperature of the blowing gas is set as 288.15 K, referring to tab. 1 for the physical parameters. As shown in fig. 4, the blowing tube intake serves as the gas inlet boundary, with the air outlet acting as the gas outlet boundary. The inlet boundary is defined as a velocity boundary condition (V) with an inlet velocity of $v = 2$ m/s. The outlet boundary is specified as a pressure boundary condition (P) with the outlet pressure set to the standard atmospheric pressure, and the gauge pressure at the outlet identified as $p = 0$ Pa. All wall surfaces are considered to adhere to no-slip wall conditions (W). In line with these boundary conditions, the finite volume method is employed to solve equations (1)-(6). A transient solver is utilized to ascertain the transient velocity field and pressure field.

Table 1. Physical properties of the protection gas

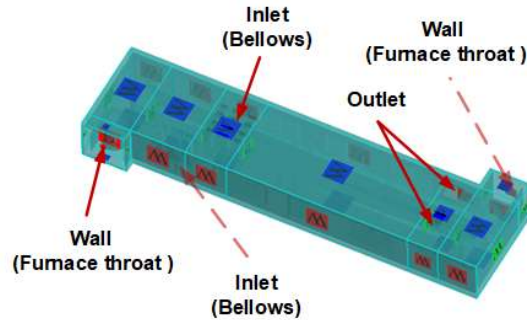| Properties	Value
Density	1.18 kg/m^3
Viscosity	1.172×10^{-5} kg/(m·s)
Temperature	288.15 K

Figure 4. Boundary conditions and the inlets and outlets

2.4. Model validation

Due to the complexity of the internal structure of the vertical continuous annealing furnace, it is very difficult and expensive to verify the model through experimental data when modeling the flow field in the annealing furnace. This research is based on the FLOW-3D software platform and employs the engineering-validated Volume of Fluid (VOF) method for free surface tracking. This algorithm accurately solves the fluid volume fraction transport equation, enabling it to precisely capture gas-liquid dynamic interface evolution [25]. Furthermore, through interface reconstruction techniques, it automatically applies physically realistic momentum boundary conditions. This characteristic grants it significant advantages in simulating industrial equipment with complex free surfaces [26]. Considering the complexity of the internal flow field of the annealing furnace, Reynolds-averaged Navier-Stokes equations were used to solve phase-averaged conservation of mass and momentum equations. This method is widely used in practical engineering problems and is capable of predicting sufficiently accurate macroscopic performance parameters [27]. Verifying the fidelity of the geometric model after mesh discretization is necessary due to the potential for geometric model distortion. A comparison between fig. 3a and fig. 3b demonstrates minimal geometric distortion before and after mesh discretization, thereby ensuring the computational accuracy of the numerical simulation.

Moreover, Qi et al. [28] analyzed the gas flow field inside the Bell-type annealing furnace using CFD. They found that the gas velocity inside the furnace first increases and then decreases, with the flow velocity at the outlet eventually stabilizing. In addition, when gas encounters right-angled boundaries inside the annealing furnace, gas reflux is inevitable. Dou et al. [29] investigated the annealing process of 3D coil cores using a CFD numerical model. The internal configuration of the annealing furnace for 3D coil cores incorporates several critical structural elements, including narrow slits, right-angled components, and cylindrical obstructions. These features bear significant resemblance to the structural characteristics observed in the overaging section of the vertical continuous annealing furnace, which constitutes the primary focus of the present study. According to their flow field results, the gas flow field becomes disordered and generates many vortices when encountering cylindrical obstacles and corners. In conclusion, the findings of the present study are consistent with the flow field characteristics of the annealing furnace with complex internal structures reported in Ref. [28, 29]. This alignment with well-established results in the literature further enhances the reliability and credibility of our conclusions.

3. Results and discussion

The computed results have been processed using the post-processing software FlowSight. The flow process and flow field characteristics of the blowing gas in the overaging section of a vertical continuous annealing furnace were analyzed and discussed. fig. 5 illustrates the transient velocity field of the blowing gas in the overaging section. Therefore, fig. 5a-d depicts the transient velocity fields of blowing gas at $t = 25$ s, $t = 50$ s, $t = 75$ s, and $t = 100$ s.

The analysis of fig. 5a indicates that at $t = 25$ s, the interior of the furnace has not been completely filled by the blowing gas. Numerous voids are observed in the flow field at the outlet and two throat sections of the furnace, showing turbulent characteristics with multiple vortices and backflows. In fig. 5b, at $t = 50$ s, it is evident that the blowing gas has filled the interior of the furnace, resulting in discernible vortices and voids generated by turbulent flow near the outlet, furnace throat, and side wall tubes. Moving on to fig. 5c, at $t = 75$ s, the flow field voids surrounding the air outlet and side wall tubes

have substantially diminished, although residual voids and vortices are still present ahead of the air outlet. Notably, the flow field near the side wall of the lower part of the furnace hearth appears deep blue, indicating that the blowing gas velocity in this area is close to zero ($v < 0.03$m/s), suggesting a stagnant state. Lastly, in fig. 5d, at $t = 100$ s, a wide range of dark blue regions ($v < 0.02$ m/s) near the outlet of the lower part of the furnace indicate that the flow effect of the blowing gas in the stagnant zone did not improve with increasing blowing time.

Upon closer comparison between fig. 5c and fig. 5d, it becomes evident that the blowing gas flow field reaches a "quasi-steady state" at $t = 75$ s, after which there is no significant change in the distribution of the flow field. Fig. 6 illustrates the streamline and flow velocity diagram of the vertical continuous annealing furnace during the over-aging stage with gas injection at $t = 100$ s. It is apparent from fig. 6 that the bellows and strip steel significantly impact the blowing gas field within the furnace. The simplified vertical continuous annealing furnace overaging section assembly model in fig. 2c demonstrates three sets of bellows, all situated in the upper half of the furnace. Consequently, the blowing gas flow rate in the upper part of the furnace is relatively sufficient, ranging from approximately 0.50 to 0.75 m/s with a higher velocity. The streamline in this region displays distinct turbulent characteristics, portraying disorderly and irregular patterns.

In the medium section of the furnace, blowing gas is divided into four longitudinally parallel flow regions by strip steels to ensure their relative independence. The streamlines of the two flow regions adjacent to the lower throat side (right side) gradually transition from irregular to orderly, while the streamlines of the two flow regions distant from the lower throat side (left side) remain chaotic and disordered. In the lower section of the furnace, the blowing gas flows parallel to the strip steel under its guidance in the two flow regions on the right side, exhibiting stable laminar flow. Subsequently, the flow line turns smoothly at the entrance of the furnace throat, and the blowing gas flows out of the furnace throat at the overaging section of the vertical continuous annealing furnace hearth. As for the two flow regions on the left side, the blowing gas hardly flows towards the furnace throat due to the obstruction of the strip steel and the guide rolls, causing the downward-flowing blowing gas to backflow upwards on the bottom surface of the furnace. Moreover, due to the significantly higher gas flow rate on the right side of the guide roller compared to the left side, the blowing gas in the right region flows downward through the gap between the guide roller and toward the left area. Upon encountering the furnace sidewall, it turns upward flowing. Consequently, there is a simultaneous upward and downward flow of blowing gas in the two flow regions on the left side, causing interference between the airflow in these two directions and resulting in a particularly severe phenomenon of cavitation in the blowing gas flow field within these two regions.

Upon comparing fig. 5c, fig. 5 d, and fig. 6, it becomes evident that recirculation zones are present at the interface between the upper and lower throats of the furnace and the sidewall once the flow field stabilizes. A detailed analysis of the furnace body structure in the aging section of the vertical continuous annealing furnace reveals that the formation of a backflow zone at the junction between the throat and sidewall during the overaging stage can be attributed to two factors. Firstly, the 90° angle between the throat and sidewall hinders gas flow, resulting in a sudden change in the direction of gas flow and horizontal backflow at this junction. Additionally, the guide rollers near the throat also partially obstruct gas inflow.
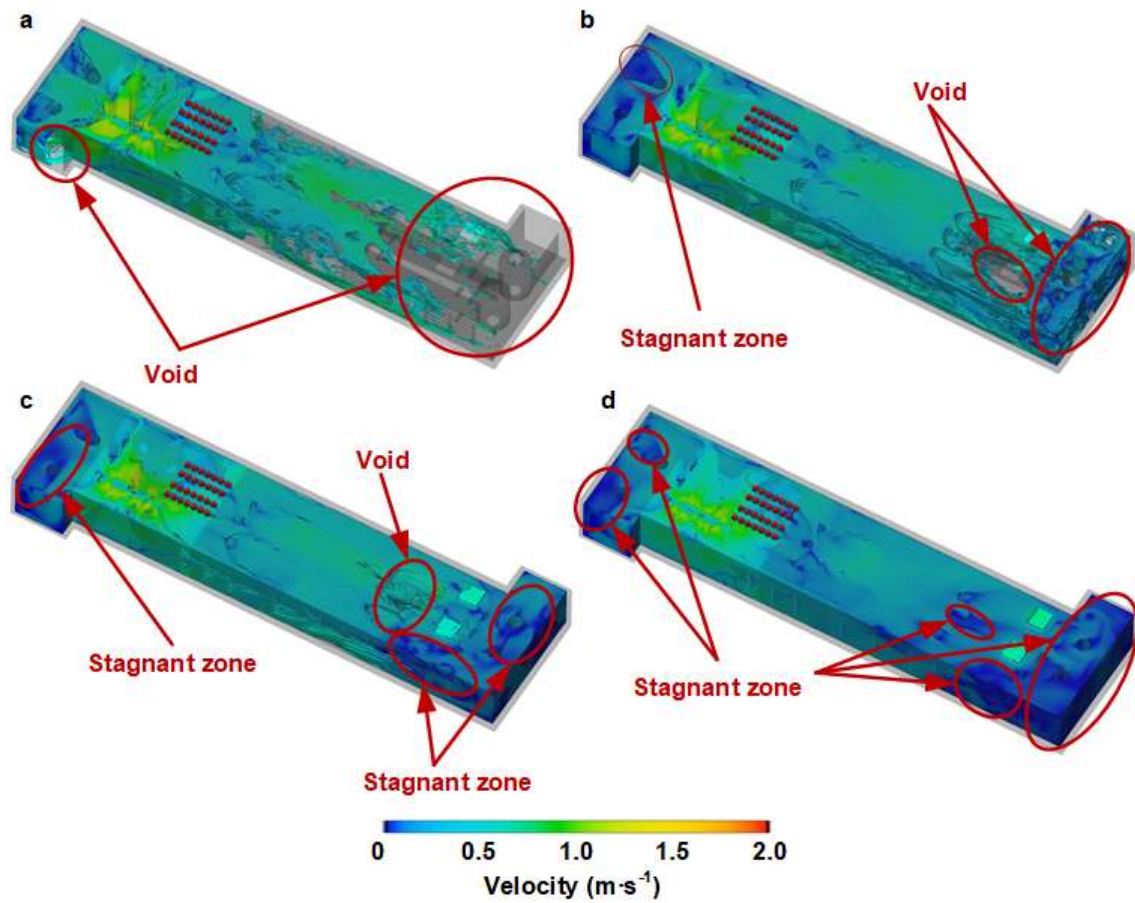
Figure 5. Transient velocity field of blowing gas in the overaging section of the vertical continuous annealing furnace: (a) $t = 25$ **s; (b)** $t = 50$ **s; (c)** $t = 75$ **s (d)** $t = 100$ **s**

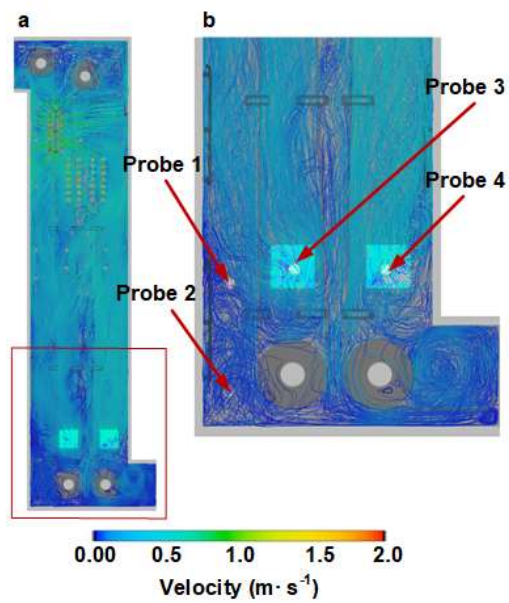**Figure 6. Flow streamlines and flow velocity of the blowing gas in the overaging section of the vertical continuous annealing furnace at** $t = 100$ **s**

In the lower section of the furnace, as illustrated in fig. 6b, four strategic probe points have been positioned to conduct a quantitative analysis of the flow velocity of the blowing gas within this specific region. Probe points 1 and 2 are situated in an area characterized by stagnant zones on one side, distanced from the throat of the furnace, while probe points 3 and 4 are located at the furnace outlet of the blowing gas. The variation of gas flow velocity at the four probe points within the time frame $t = 25 - 100$ s is presented in fig. 7. From fig. 7a and b, it can be observed that the gas flow velocity at probe points 1 and 2 remains essentially constant after $t = 75$ s, indicating that the flow field has reached a "quasi-steady state," which is consistent with the results obtained from fig. 5c and fig. 5d cited earlier. Specifically, as shown in fig. 7a, it can be seen that before $t = 75$ s, the flow velocity of the blowing gas at probe point 1 fluctuates between 0 - 0.4 m/s, indicating an unstable flow field. After $t = 75$ s, the flow velocity of the blowing gas fluctuates between 0 - 0.1 m/s and eventually approaches 0.05 m/s. Combined with fig. 6b, it is known that when the flow field of the blowing gas reaches a quasi-steady state, a turbulent vortex around probe points 1 and 2 exists due to obstruction from the support frame below them. Therefore, the flow velocity of the blowing gas at probe points 1 and 2 is close to zero, forming a stagnant zone of flow motion. Moreover, according to fig. 7, before $t = 75$ s, the blowing gas flow rate at probe points 1 and 2 fluctuates and decreases between 0.075 - 0.175 m/s. Subsequently, after $t = 60$ s, the gas flow velocity fluctuated between 0 - 0.4 m/s during blowdown and gradually converged towards approximately 0.05 m/s. The streamlines around probe points 3 and 4 exhibit higher density, indicating an elevated gas velocity at the outlet, as observed from fig. 6, fig. 7c, and fig. 7d. Notably, during the time interval of $t = 50 - 100$ s, significant fluctuations in blowing gas velocity occur at probe points 3 and 4. Eventually, a stable value of approximately 0.2 m/s is attained. This behavior can be attributed to the smaller cross-sectional area and denser streamlines present at the outlet, resulting in an increased velocity that adheres to mass and momentum principles.
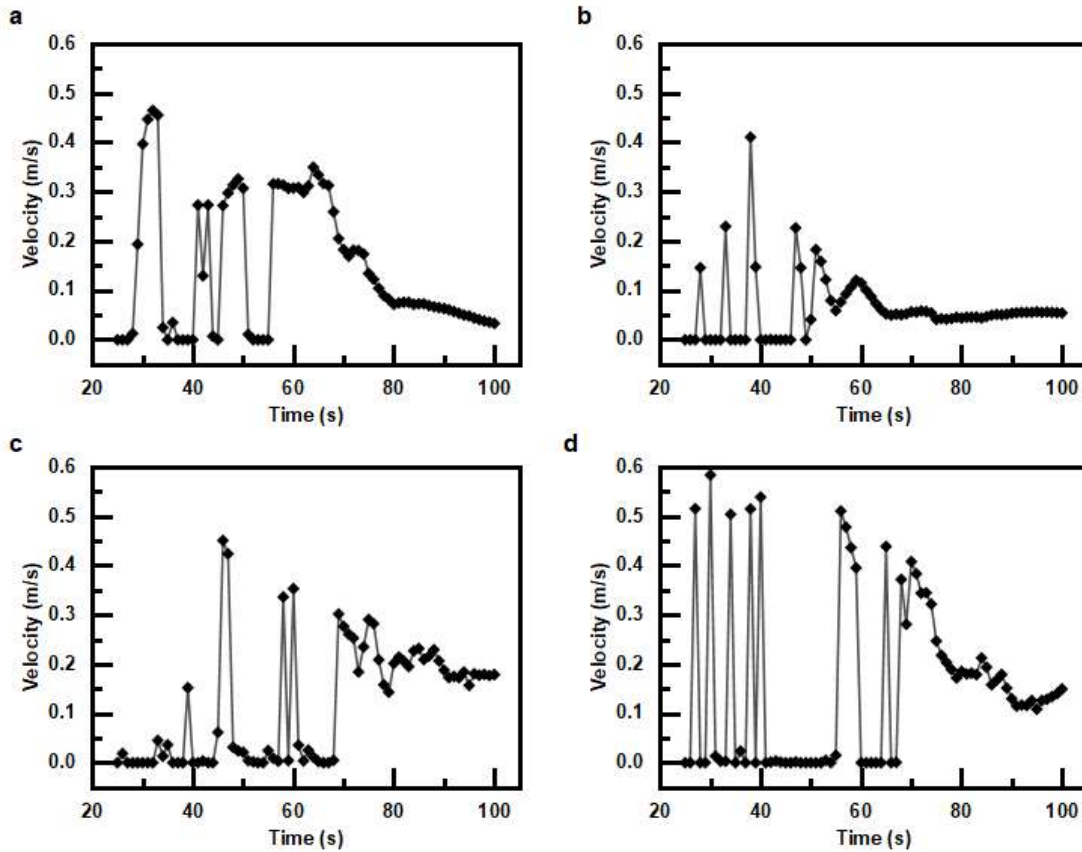
Figure 7. Flow velocity of the blowing gas at the four probe points in the overaging section of the vertical continuous annealing furnace varying with the time of t = 20 - 100 s: (a) probe point #1, (b) probe point #2, (c) probe point #3, and (d) probe point #4

4. Conclusion

Given the conflicting demands posed by the large size of the annealing furnace and the influence of the CFD numerical model mesh on computational efficiency, we have opted to simplify the geometric model. Nonetheless, we have made sure to retain the key dimensions and characteristics of the annealing furnace. The flow field of the blowing gas in the overaging section of a vertical continuous annealing furnace model was numerically analyzed in this article. The main conclusions are as follows.

The blowing gas flow field reaches a "quasi-steady state" around t = 75 s. After this point, the flow field void and flow stagnant zone in the furnace do not visibly improve with increased blowing time.

In the upper region of the furnace, where the bellows are located, the gas flow rate is fast, achieving thorough blowing, and exhibits typical turbulent characteristics. However, in the middle and lower parts of the furnace, the flow is divided into four relatively independent regions by the strip steel. In two of these regions near the lower throat side (right side), the gas flow transitions from disorderly to orderly, forming stable laminar flow parallel to the downward movement of the strip steel, which improves the blowing effect. However, in two flow areas on the side (left side) away from the lower throat, the blowing gas cannot flow smoothly out of these areas, leading to large-scale flow field voids and stagnant zones that seriously affect the blowing effect. Localized flow field voids and stagnant zones

are also found near components and structures such as guide rolls, side wall pipes, and support frames, further affecting the flow of blowing gas.

Due to the obstruction caused by the gas flow turning abruptly at a 90° angle when entering other working sections of the furnace throat, there is a certain amount of backflow at the entrance of the furnace throat.

These insightful research findings can serve as a valuable framework for subsequent investigations aimed at optimizing furnace structure and enhancing blowing efficiency in vertical continuous annealing furnaces.

Acknowledgments

Reference

[1]   Wan F, Wang YQ., et al., Modeling of Strip Heating Process in Vertical Continuous Annealing Furnace, *Journal of Iron and Steel Research International, 19* (2012), 5, pp. 29-36

[2]   Mayrhofer, Michael K., et al., CFD Investigation of a Vertical Annealing Furnace for Stainless Steel and Non-ferrous Alloys Strips – A Comparative Study on Air-staged & MILD Combustion, *Thermal Science and Engineering Progress*, *28* (2022), 5, pp. 101056

[3]   Pradhan, R., and Melcher, E. D., Characteristics of High-Strength Cold-Rolled Sheet Steels Produced by Continuous Annealing. *SAE Transactions*, *93* (1984), pp. 81–89

[4]   Bleck, W., et al., Recrystallization and Mechanical Properties of Microalloyed Cold-rolled Steel, *Materials Technology*, *59* (1988), 6, pp. 344-351

[5]   Khan, N.Z., et al., Steel Heat Treatment: Equipment and Process Design, CRC Press, USA, Boca Raton, 2006

[6]   Gao, P., et al., Optimal Reynolds Number of Cooling Water in Conformal Cooling Molds, *Applied Thermal Engineering*, *236* (2024), 5, pp. 121509

[7]   Mohrbacher, H., et al., Annealing Response and Yielding Behavior of Cold Rolled Advanced HSLA Steels, *Materials Science and Engineering A*, *903* (2024), 9, pp. 146666

[8]   Ray, R.K., et al., "Back-annealing" of Cold Rolled Steels Through Recovery and/or Partial Recrystallisation, *International Materials Reviews*, *56* (2011), 2, pp. 73-97

[9]   Wan, F., et al., Modeling of Strip Temperature in Rapid Cooling Section of Vertical Continuous Annealing Furnace, *Journal of Iron and Steel Research International*, *19* (2012), 11, pp. 27-32

[10]   Hajaliakbari, N., Hassanpour, S., Analysis of Thermal Energy Performance in Continuous Annealing Furnace, *Applied Energy*, *206* (2017), 4, pp. 829-842

[11]   IMOSE, M., Heating and Cooling Technology in The Continuous Annealing, *Transactions of the Iron and Steel Institute of Japan*, *25* (1985), 9, pp. 911-932

[12]   Chen, T.C., et al., 3-D Temperature and Stress Distributions of Strip in Preheating Furnace of Continuous Annealing Line, *Applied Thermal Engineering*, *30* (2010), 8, pp. 1047-1057

[13]   Colla, V., et al., Prediction of Continuous Cooling Transformation Diagrams for Dual-phase Steels from the Intercritical Region, *Metallurgical and Materials Transactions A*, *42* (2011), 9, pp. 2781-2793

[14]   Shi, Y.L., et al., Effects of Prandtl Number on Impinging Jet Heat Transfer under a Semi-Confined Laminar Slot Jet, *The International Communications in Heat and Mass Transfer*, *30* (2003), 4, pp. 455-464

[15]   Han, S.H., et al., Numerical Analysis of Heating Characteristics of a Slab in a Bench Scale Reheating Furnace, *International Journal of Heat and Mass Transfer*, *50* (2007), 9, pp. 2019-2023

[16]   Chen, K., et al., Inverse Parameter Identifications and Forward Strip Temperature Simulations of the Continuous Annealing Line with Physics-informed Neural Network and Operation Big Data, *Engineering Applications of Artificial Intelligence*, *127* (2024), 12, pp. 107307

[17]   Zareba, S., et al., Mathematical Modelling and Parameter Identification of a Stainless Steel Annealing Furnace, *Simulation Modelling Practice and Theory*, *60* (2016), 10, pp. 15-39

[18]   Li, C.S., et al., Microstructure and Mechanical Properties of Dual Phase Strip Steel in the Overaging Process of Continuous Annealing, *Materials Science & Engineering A*, *627* (2015), 12, pp. 281-289

[19]   Cai, X., et al., Process Design and Prediction of Mechanical Properties of Dual Phase Steels with Prepositional Ultra Fast Cooling, *Materials and Design*, *53* (2014), 7, pp. 998-1004

[20]   Calcagnotto, M., et al., Deformation and Fracture Mechanisms in Fine- and Ultrafine-grained Ferrite/Martensite Dual-phase Steels and the Effect of Aging, *Acta Materialia*, *59* (2011), 2, pp. 658-670

[21]   Lin, K., et al., Effect of Annealing Atmosphere and Steel Alloy Composition on Oxide Formation and Radiative Properties of Advanced High-strength Steel Strip, *Metallurgical and Materials Transactions B*, *53* (2022), 1, pp. 380-393

[22]   Flow Science, Inc. Flow-3D V11.2 Documentation. 2016

[23]   Seeta Ratnam, G., Vengadesan, S., Performance of Two Equation Turbulence Models for Prediction of Flow and Heat Transfer over a Wall Mounted Cube, *International Journal of Heat and Mass Transfer*, *51* (2008), 11, pp. 2834-2846

[24]   Nesbitt, T.S., et al., The Prediction of Laminarization with a Two-equation Model of Turbulence, *International Journal of Heat and Mass Transfer*, *15* (1972), 4, pp. 301-314

[25]   C.W Hirt, B.D Nichols, Volume of Fluid (VOF) Method for the Dynamics of Free Boundaries, *Journal of Computational Physics*, *39* (1981), 1, pp. 201-225

[26]   J.U Brackbill, D.B Kothe, et al., A Continuum Method for Modeling Surface Tension, *Journal of Computational Physics*, *100* (1992), 2, pp. 335-354

[27]   A.G. Straatman, R.J. Martinuzzi, A Study on the Suppression of Vortex Shedding from a Square Cylinder Near a Wall, *Engineering Turbulence Modelling and Experiments 5*, (2002), 3, pp. 403-411

[28]   Qi WD, Song J, et al., Analysis on Gas Flow Field in Bell-type Annealing Furnace by Using FLUENT, *Applied Mechanics and Materials*. *345* (2013), 5, pp. 581–585

[29]   R. Dou, H. Zhao, et al., Numerical Model and Optimization Strategy for the Annealing Process of 3D Coil Cores, *Applied Thermal Engineering*. *178* (2020), 5, pp 115517